JOURNAL OF GEOPHYSICAL RESEARCH, VOL. 113, D14S04, doi:10.1029/2007JD009582, 2008

The strongest desert dust intrusion mixed with smoke over the Iberian Peninsula registered with Sun photometry

V. E. Cachorro,[1] C. Toledano,[1,2] N. Prats,[1] M. Sorribas,[3] S. Mogo,[1,4] A. Berjón,[1] B. Torres,[1] R. Rodrigo,[1] J. de la Rosa,[5] and A. M. De Frutos[1]

Received 7 November 2007; revised 4 March 2008; accepted 10 April 2008; published 17 July 2008.

[1] We present the analysis of the strongest North African desert dust (DD) intrusion that occurred over the Iberian Peninsula (IP) during the last decade, as registered by modern remote sensing techniques like Sun photometry. This event took place from 22 July to 3 August 2004. The most relevant features of this exceptional event, originated over the Saharan desert, were its great intensity and duration. We focus on the columnar aerosol properties measured by the AERONET-Cimel photometers at El Arenosillo (southwest) and Palencia (north-center) stations. Aerosol optical depth (AOD) reached a maximum of 2.7 at El Arenosillo during 22 July and 1.3 at Palencia on 23 July, with the Ånsgtröm exponent values near zero during the AOD peaks. In addition, PM10 concentration levels are also reported at various sites of the IP in order to establish the impact of this intrusion, reaching daily values as high as 200 $\mu g/m^3$ and peaks near 600 $\mu g/m^3$ in an hourly basis. The interest of this special event is increased because of the mixing with smoke particles from concurrent forest fires in the IP. Features of the columnar volume particle size distribution and derived microphysical parameters, the single scattering albedo, and a reliable estimation of the radiative forcing under these extreme conditions are also reported. Complementary information, as air mass back trajectories, synoptic charts, images, and AOD maps of satellite sensors (SeaWIFS, MODIS) together with NAAPS prognostic model, is used in the analysis in order to draw a detailed scenario of this dust-smoke event over the IP.

Citation: Cachorro, V. E., C. Toledano, N. Prats, M. Sorribas, S. Mogo, A. Berjón, B. Torres, R. Rodrigo, J. de la Rosa, and A. M. De Frutos (2008), The strongest desert dust intrusion mixed with smoke over the Iberian Peninsula registered with Sun photometry, *J. Geophys. Res.*, *113*, D14S04, doi:10.1029/2007JD009582.

1. Introduction

[2] The Sahara and Sahel desert areas are the main source of mineral aerosols in the northern hemisphere [*Prospero et al.*, 2002; *Ginoux et al.*, 2004]. The transported mineral aerosols directly affect extensive areas over Europe. However, the apportioning and impact of the desert aerosol on the total aerosol load in Europe still very uncertain. Therefore the Saharan dust has been intensively investigated in the last years [see *Goudie and Middleton*, 2001, and references therein], with special attention to the absorption properties and the radiative forcing [*Sokolik et al.*, 2001; *Tanré et al.*, 2003; *Myhre et al.*, 2003].

[3] Because of its geographical position near the North African continent, the Iberian Peninsula is frequently affected by African air masses loaded of mineral dust particles. These intrusions entail the episodes with largest aerosol load over the IP, in such a way that they modulate the aerosol climatology in different areas of the IP, especially in the south [*Toledano et al.*, 2007a, 2007b]. Although in southern Spain, desert dust intrusions are more frequent than in the northern areas, these areas also have a high aerosol load as can be seen analyzing the data of Palencia station [*Rodrigo*, 2007]. Note also that dust event affecting the southeastern and southwestern areas of Spain follow different patterns [*Escudero et al.*, 2005]. African desert dust plumes crossing the North Atlantic often touch the Galicia (northwestern) coasts, with a peculiar pattern which does not affect other areas of the IP.

[4] Desert dust (hereafter DD) events are known in Spain for centuries, but only recently the remote sensing techniques allow an adequate quantification of these phenomena. Some studies have been carried out for a quantitative evaluation over long periods (more than 20 years) based on wet deposition, the so-called red rains [*Avila et al.*, 1997; *Avila*, 1999, and references therein]. *Avila* [1999] defines the desert intrusions over the IP as sporadic and irregular. A

[1]Group of Atmospheric Optics, University of Valladolid, Valladolid, Spain.
[2]Now at Meteorological Institute, University of Munich, Munich, Germany.
[3]Estación de Sondeos Atmosféricos El Arenosillo, Earth Science Division, National Institute for Aerospace Technology, Mazagón, Spain.
[4]Now at Departamento de Fisica, Universidad da Beira Interior, Covilhã, Portugal.
[5]Department of Geology, University of Huelva, Huelva, Spain.

0148-0227/08/2007JD009582$09.00

study based on the combination of PM10 time series, satellite images, aerosol modeling and back trajectories together with wet deposition carried out by *Escudero et al.* [2005] allowed a first reliable evaluation of mineral dust intrusions over the eastern IP.

[5] Recently, we have carried out an inventory of DD intrusions over the southwestern IP based on Sun photometer data obtained at El Arenosillo AERONET site [*Toledano et al.*, 2007b]. This inventory provides a more accurate evaluation of the contribution and impact of desert dust aerosols to the total aerosol load (both columnar and ground level) in the IP. A similar analysis may be carried out for other areas of Europe, obviously by means of Sun photometer, PM10 or other type of data. For instance, Lidar data are reported by *Mona et al.* [2006]. In the work by *Escudero et al.* [2006] a methodology based on the HYSPLIT model is developed and applied to evaluate the contribution of African dust source areas to the PM10 concentration in the central IP.

[6] The most frequent intrusions over de IP take place under clear sky or partly cloudy conditions (as this is the most frequent meteorological scenario in Spain). The dry deposition of dust aerosols is therefore the most important deposition mechanism, although the wet deposition must be also taken into account. The relative contribution of the wet deposition phase with respect to the dry deposition, although very variable, is about 10–15%, according to the data reported in the two above mentioned inventories [*Escudero et al.*, 2005; *Toledano et al.*, 2007b] and the data reported by *Avila* [1999].

[7] In this work, we present the characteristics of one of the strongest DD episode registered over the IP in the last decades and the strongest in the last 8 years. This assertion is based on the DD inventory by *Toledano et al.* [2007b], and also on the PM10 database recorded by the Air Quality Network of Andalusia Government (QNAG) and the EMEP (Cooperative Program for Monitoring and Evaluation of the Long Range Transmission of Air Pollutants in Europe) stations in Spain. The reason to study this episode in detail comes from the necessity to characterize and quantify the desert aerosols over the IP and their impact in terms of aerosol mass, both in the atmospheric column and at ground level.

[8] In summer the occurrence of forest fires in the IP is very high because of the dry soil-air conditions and the high temperatures. The impact and evaluation of smoke aerosol must be accounted for at least at a regional scale. The DD event reported here extended over large areas and lasted many days, what resulted in its mixing with biomass burning (BB) aerosols over different areas of the IP. The optical properties of the mixture also vary in a regional scale.

[9] The sites of measurements and the instrumentation utilized in this work are described in section 2. The experimental method is summarized in section 3. In the results (section 4) the intensity and duration of this DD-smoke episode based on AOD-α values, satellite and model data (section 4.1) and PM10–2.5 levels at various stations (section 4.2) are described. The synoptic and meteorological scenario is described in section 4.3 and section 4.4 provides detailed information about the range of values defining the main columnar physical-optical properties of ''pure'' desert and mixed (dust + smoke) aerosols over two representative sites: Palencia (north) and El Arenosillo (south). The discussion about the aerosol radiative forcing during this episode is also of interest for regional climate studies (section 4.5). Finally the conclusions are described in section 5.

2. Sites of Measurements and Instrumentation

[10] The analysis of this particular event will be carried out on the basis of several types of data: Sun photometer observations, satellite data, aerosol concentration at ground level (PM2.5, PM10) and meteorological charts. The measurement sites and instruments are described in this section.

[11] The most important data for this analysis are provided by the Cimel Sun-sky radiometers (model CE-318). Two Cimel instruments, included in the AERONET network [*Holben et al.*, 1998] operate in El Arenosillo, located in southwestern Spain, and Palencia, located in north-central Spain (Figure 1a). These instruments perform direct Sun measurements and also sky radiance measurements in the solar almucantar and principal plane configurations (for details about the instrument see *Holben et al.* [1998] and the AERONET web page). A description of the aerosol climatology at El Arenosillo site is given by *Toledano et al.* [2007a]. The AOD values during typical conditions and during typical desert dust events are reported there, as well as the frequency and seasonality of the dust episodes.

[12] Different data provided by MODIS (Moderate Resolution Imaging Spectroradiometer, http://modis.gsfc.nasa.gov) are also used in the analysis, both from Terra and Aqua satellite platforms: true color images, aerosol optical depth and the fire maps provided by the MODIS Rapid Response System (http://rapidfire.sci.gsfc.nasa.gov). True color images from SeaWIFS (Sea-viewing Wide Field of view Sensor, http://oceancolor.gsfc.nasa.gov/SeaWiFS) have also been analyzed.

[13] The levels of particulate matter PM10 and PM2.5 in remote areas during dust events are very relevant, because they represent the extreme values measured in the south of Europe. The ground concentrations also permit the evaluation of the impact of these events over urban areas [*Rodriguez et al.*, 2001, 2002; *Querol et al.*, 2004, 2008]. The importance of these measurements is also related to the EU directives for air quality. The detailed analysis of aerosol properties at ground level [*Sorribas et al.*, 2006] and chemical identification [*González et al.*, 2007] will need a separate analysis.

[14] PM10 and PM2.5 concentrations are therefore analyzed, daily filter gravimetric mass analysis obtained with low-volume impactors, at two remote stations in the IP (Figure 1a): Peñausende, located in the northwest near the Portugal border, a remote site belonging to Castilla y León Autonomous Government; and Campisabalos in the east-center of the IP, belonging to Castilla la Mancha Autonomous Government. Both stations belong to the EMEP network managed by the Spanish Ministry for Environment (Ministerio de Medio Ambiente). PM10 from two more sites, Valladolid and Palos de la Frontera, is also analyzed by means of automatic hourly beta attenuation measurement. In this case, the data correspond to polluted places. The first one is located in the north and the data belong to

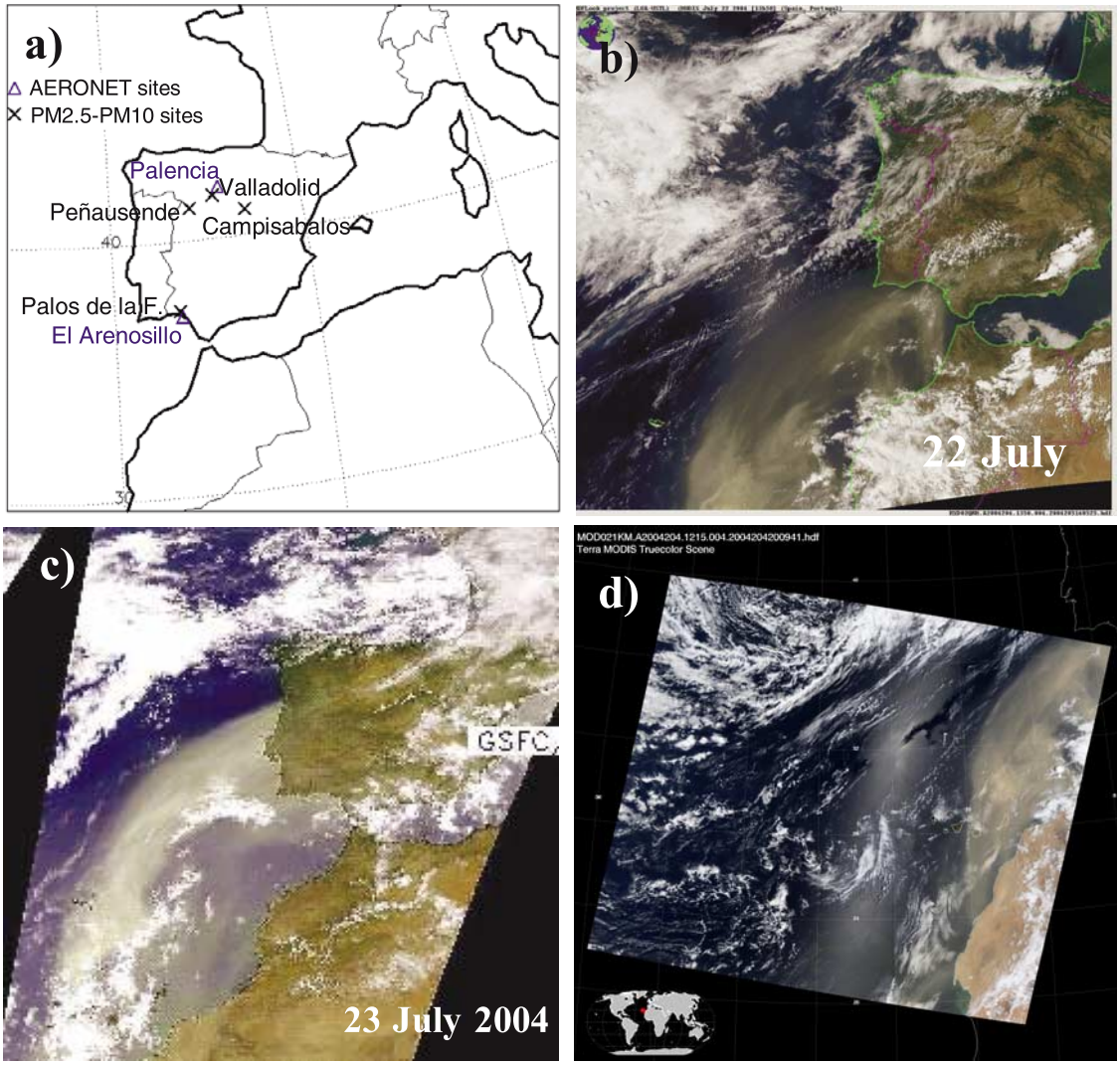

Figure 1. (a) Location of the sites of measurements. (b) MODIS-Aqua image on 22 July 2004 at 1350 UTC. (c) SeaWIFS image for 23 July 2004 at 1200 UTC. (d) MODIS-Terra image on 22 July 2004 at 1215 UTC.

the Urban Air Quality Network of Valladolid town. This town is 45 km south of Palencia and 100 km east of Peñausende, being representative of a medium-size town in Spain, with continental climate. The selected station in the south, Palos de la Frontera, is 8 km away from El Arenosillo station but inside the industrial belt of the town of Huelva.

3. Experimental Method

[15] From the Sun photometer direct Sun measurements, the aerosol optical depth (AOD) at selected spectral channels is derived, following the well-known Beer-Bouguer-Langley law. In the Cimel Sun photometer four wavelengths (440, 670, 870 and 1020 nm) are used for aerosol investigation [*Holben et al.*, 1998]. The Ångström exponent (α) is derived according to the Ångström power law, using the 440, 670 and 870 nm channels [*Cachorro et al.*, 1987; *Eck et al.*, 1999]. The data are processed within the AERONET version 2 direct Sun algorithm, which is described on detail in the AERONET web page. These data define the aerosol climatology of the site [*Holben et al.*, 2001].

[16] From the almucantar sky radiance measurements at these same four wavelengths, and the corresponding AOD values as well, an inversion algorithm (AERONET version 2 [*Dubovik and King*, 2000; *Dubovik et al.*, 2002, 2006]) retrieves a large set of optical and microphysical aerosol parameters: columnar volume particle size distribution, median radius, effective radius, volume concentration (for total, fine and coarse modes), refractive indices (real and imaginary parts), single scattering albedo (SSA), phase function and asymmetry parameter as a function of wavelength, sphericity, etc. The evaluation of the sphericity is an important improvement of the version 2 AERONET inversion. Aerosol particles are assumed to be partitioned into two components: spherical (polydisperse, homogeneous spheres) and nonspherical (mixture of polydisperse, randomly oriented homogeneous spheroids following the aspect ratio distribution retrieved by *Dubovik et al.* [2006]). The retrieval provides the percentage of nonspherical particles

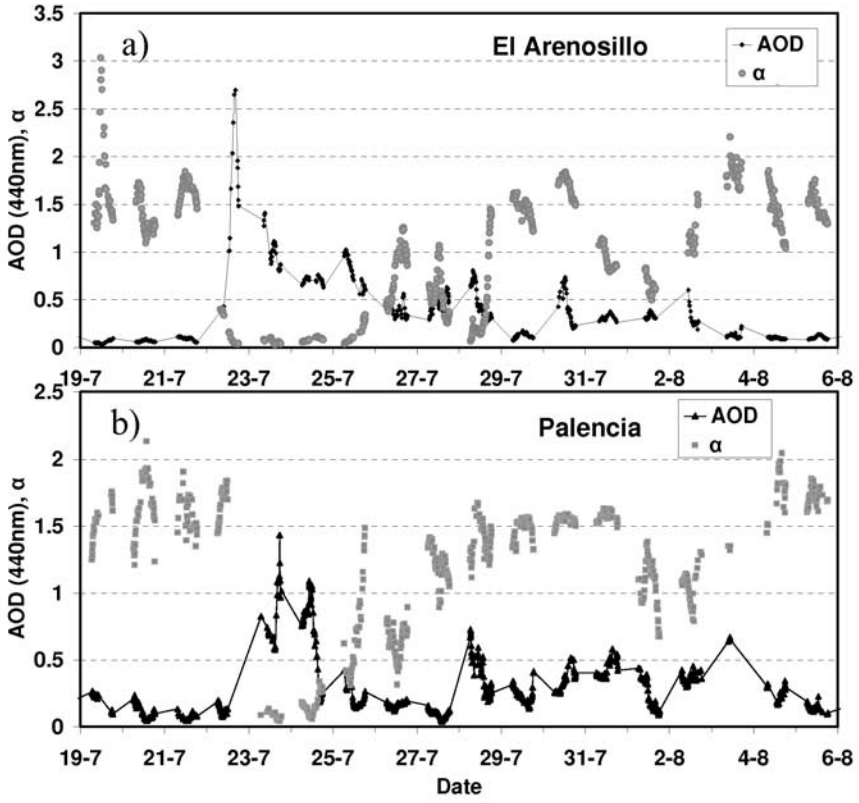

Figure 2. Time series of the AOD (440 nm) and the Ångström exponent (α) at El Arenosillo and Palencia during the dust-smoke episode, from 19 July to 6 August 2004.

in the observed aerosol [*Dubovik et al.*, 2006]. Some of the parameters provided by AERONET, like the SSA and radiative forcing, may be used carefully [*Dubovik et al.*, 2002, 2006]. Detailed description about the conditions, criteria and errors in our analysis of the optical and microphysical aerosol products is given by *Prats et al.* [2008].

[17] The methodology followed in the analysis of this event is similar to that used by different authors for other case studies [*Cachorro et al.*, 2006; *Perez et al.*, 2006; *Pinker et al.*, 2001; *Lyamani et al.*, 2006]. The AOD, currently used for monitoring this type of events, gives information about the aerosol load in the whole atmospheric column over the site. It will be compared with the particulate matter concentration at ground level, i.e., PM2.5/PM10 data. Although a relatively strong correlation may exist between both data sets, they do not follow necessarily the same temporal evolution, because of the different development of the processes of transport and deposition of particles. Therefore, both types of data will be used in a complementary basis, as the most powerful tool for showing the intensity of the event and retrieving consistent information.

[18] In the description of the event, we also make use of back trajectories, calculated with the HYSPLIT model [*Draxler and Rolph*, 2003; *Rolph*, 2003], and the synoptic charts of FNL [*Stunder*, 1997] NOAA's meteorological archive. Five day (120 h) back trajectories are calculated at 00, 06, 12 and 1800 UTC for El Arenosillo and Palencia, at three different heights (500, 1500 and 3000 m asl). For the vertical motion, the model vertical velocities are used.

4. Results

4.1. AOD and Ångström Exponent Values

[19] This special DD episode is characterized by its extreme intensity and duration affecting the entire IP. In Figures 1b, 1c, and 1d, three satellite images illustrate the position and extension of the dust plume. The intensity of the event can be quickly envisaged. Figure 1b corresponds to the MODIS image on 21 July, when the plume reached the south of Portugal and the Gulf of Cadiz, where El Arenosillo station is located. Figure 1c shows the SeaWIFS image on 22 July, where we can observe the Atlantic Arc described by the dust plume, which follows a W–E direction in northern areas of the IP.

[20] Despite these illustrative images, we need to document the intensity of this DD outbreak by means of a physical quantity. Therefore we present the temporal evolution of the AOD and the Ånsgtröm exponent (α) over the two selected AERONET sites, El Arenosillo and Palencia (Figure 2), as well as the MODIS aerosol optical depths over the IP (Figure 3). Figure 2a shows the quick arrival of the desert plume at both stations (the AOD increases extraordinarily from one day to the next), during the early morning of 22 July at El Arenosillo and 23 July at Palencia. This information is also confirmed by the analysis of air mass back trajectories, as it will be shown later. The highest AOD (440 nm) is registered precisely on the first day of the

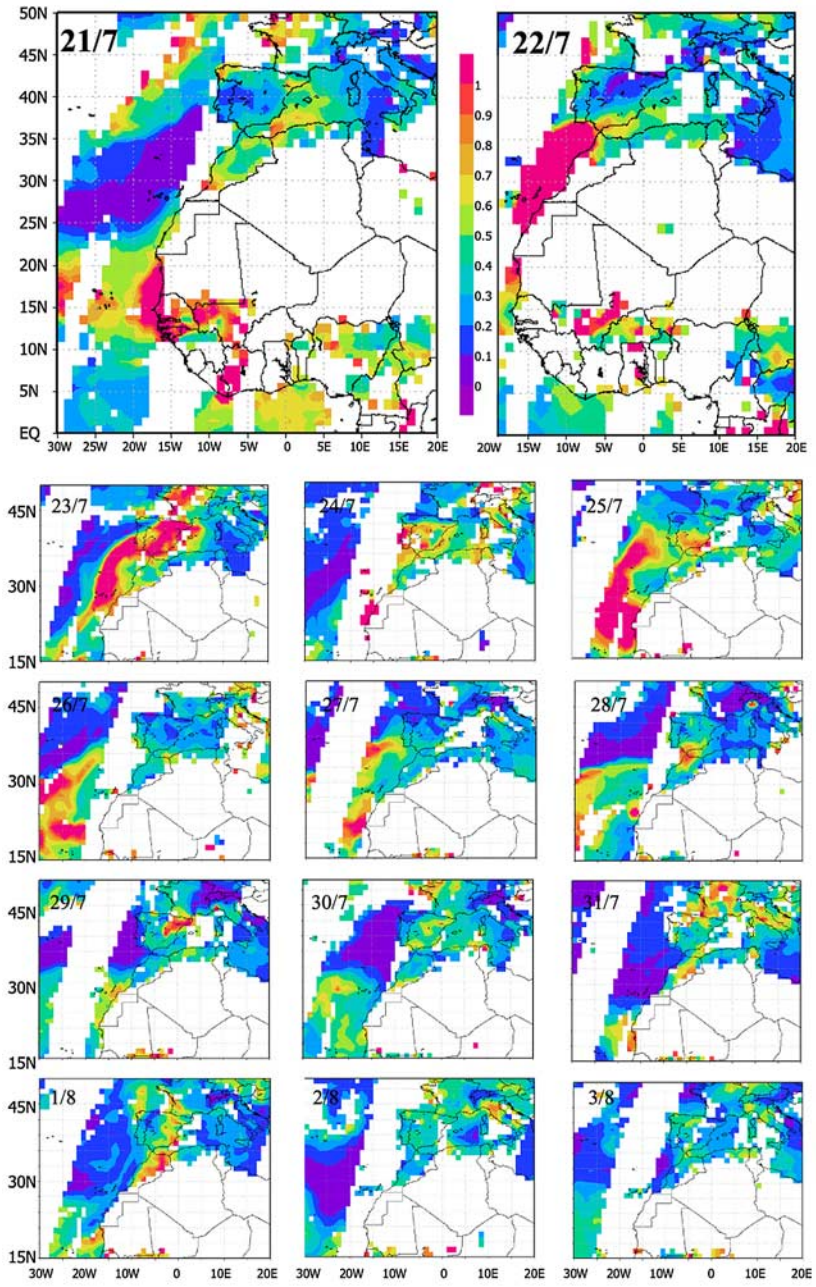

Figure 3. Daily plots of the AOD at 550 nm provided by Terra-MODIS from 21 July to 3 August 2004 over a wide longitude-latitude area to observe the evolution of the desert dust plume.

event at the southern station (22 July) with a value of 2.7. The following days 23–25 July show a clear desert aerosol character. The maximum level of AOD at the northern station of Palencia is 1.5, also obtained during the first day of the dust layer arrival, 23 July. On 24 July a well established desert aerosol type is measured, but the desert plume quickly moved away, as shown by the AOD, which dropped back to background levels on 27 July. These AOD peaks are the highest registered in both stations, where the mean AOD (440 nm) are 0.17 (El Arenosillo) and 0.1 (Palencia).

[21] In Figure 2 we can also observe the time series of the Ångström exponent, which shows very low values (near zero), in inverse correspondence with the high AOD for desert aerosols. One of the characteristics of the DD episodes is the high variability shown by both parameters, not only through the entire period but also during each day. As can be seen in Figure 2, the episode is nearly uncontaminated by clouds in spite of its long duration. Only on 22–23 July at El Arenosillo and 22–25 July at Palencia, partial cloudiness is observed and some data were removed by the AERONET cloud-screening algorithm.

[22] Although the information given by Figure 2 is very important, it is restricted to local stations and does not provide global spatial coverage, as the satellite images do. The satellite data have proved to be suitable for the

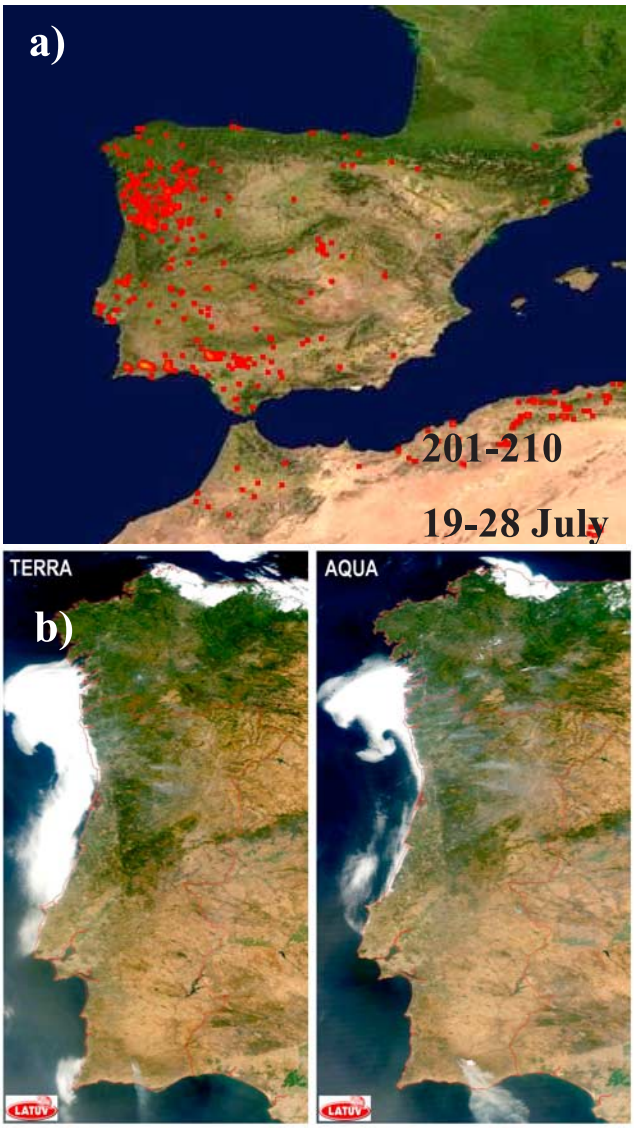

Figure 4. (a) Number of fires (hot spots) over the IP in the period 19–28 July given by the MODIS Rapid Response System. (b) Aqua and Terra MODIS images illustrating the evolution of the forest fire plumes over the west Iberian Peninsula on day 27 July (note there is a delay between both overpasses).

observation of the Saharan dust, especially over the ocean [*Kaufman et al.*, 2001; *Prospero et al.*, 2002; *Chiapello et al.*, 2005; *Kaufman et al.*, 2005]. The global spatial picture over the entire IP together with the path of the desert plume from its origin in the African continent is shown by means of the AOD maps generated by the MODIS-Giovanni facility. Figure 3 is a composite following the MODIS-AOD day-to-day evolution, from 15°N to 45°N latitude and 30°W to 20°E longitude. On 21 July the IP is free of desert aerosols and the plume is located over the western Sahel and the coasts of Mauritania, Senegal and Guinea. On 22 July a strong and wide plume extends from the Sahara to the southern IP, exactly when the highest AOD was obtained at El Arenosillo. During the early morning on 23 July the intrusion reaches the north of the IP and covers practically the whole IP (only the northwest appears to be less influenced). Because of the extent of the plume, it penetrates from the west and the south at the same time. The episode lasts many days, with the highest AOD values during 22–25 July, as reported in both Figures 2 and 3. However, it is difficult to define the end of the episode, not only because of the intrinsic variability but for the mixing with smoke and the recirculation processes, which prevail during the summer in the IP [*Millán et al.*, 1997; *Garcia-Herrera et al.*, 2005].

[23] The DD was mixed with smoke from the forest fires that affected both stations: the fires in the north and south of Portugal and also the big forest fire occurred in the Sierra de Aracena, 50–70 km far from El Arenosillo station, from 27 July to 4 August, with up to 60000 Ha burned from which 30000 Ha corresponded to forest. Figure 4 is illustrative of the high number of fires over the IP (hot spots in Figure 4a, which corresponds to the period 19–28 July). The extension and direction of the smoke plumes can be observed in the true color composite MODIS image (Figure 4b). The mixture of smoke and the background aerosols with the desert dust over the western IP is a main feature in this case [*Pace et al.*, 2005, 2006].

[24] These peculiarities are well documented by the variability of the Ånsgtröm exponent in Figure 2. The quick changes in this parameter show the change in predominance from DD (low α) to BB (high α). This means that a mixture of DD and BB aerosols was present almost all the time. Observing Figure 2a, the quick strong increase of the α values on 26 July (up to 1.0) indicates the reduction of the dust concentration and the influence of the forest fires in south Portugal (area of Faro), which continues on 27 and 28 July. However, on 28 July new dust is observed in the MODIS and Sun photometer data (decrease in the Ångström exponent). The influence of the smoke from Sierra de Aracena fire intensifies again during the afternoon (Ångström exponent increases through the day). It might be considered that on 29 July the desert smoke episode is finished because the AOD-α comes near to typical summer background values (maximum of AOD is 0.17 and α = 1.6 on this day) but the data through the next days clearly show that the DD-BB situation persists and extends to 3 August. The Sierra de Aracena forest fire lasted until 4 August according to local information.

[25] The areas of northern Spain (Palencia) were also affected by smoke, in this case by the forest fires in north Portugal (Figure 4). Observing Figure 2b, we can see that the AOD values fall during 25 to 27 July as the DD event decays, being the AOD values on 27 July those of normal summer conditions, which seem to indicate the final of the desert episode. However, we must note that in the afternoon of 25 July the Ånsgtröm exponent shows a quick increase which may be due to the arrival of smoke, whereas on 26 July α shows a new decrease due to some dust still remaining in the area (see also Figure 3). Again, the quick increase of the AOD (0.7 in the morning) with high associated α values on day 28 may be due to smoke as we can see in more detail in the next Figures 4 and 5. From days 28 July to 3 August there is a mixture of smoke and mineral dust (see days 3 and 4 August in Figures 3 and 5). It must also be considered the influence of the prevailing continental background aerosols, with Ångström exponent

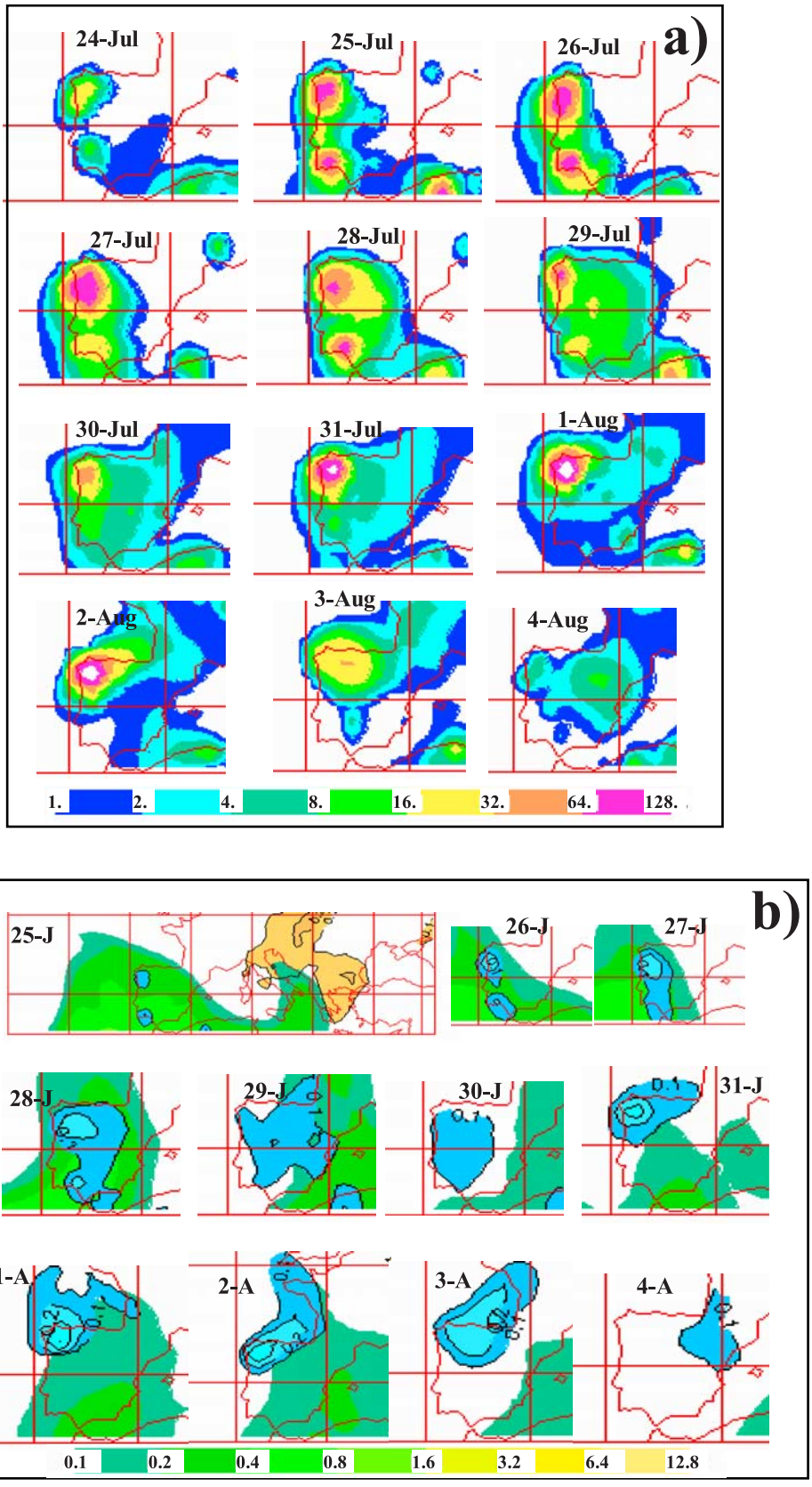

Figure 5. (a) Daily plots at 1200 UTC of smoke surface concentration (in $\mu g/m^3$) provided by the NAAPS model over the IP from 24 July to 4 August 2004. (b) Daily plots of the AOD at 550 nm for desert dust (green color scale) and smoke particles (blue colors) given by the NAAPS model over the IP from 25 July to 4 August 2004.

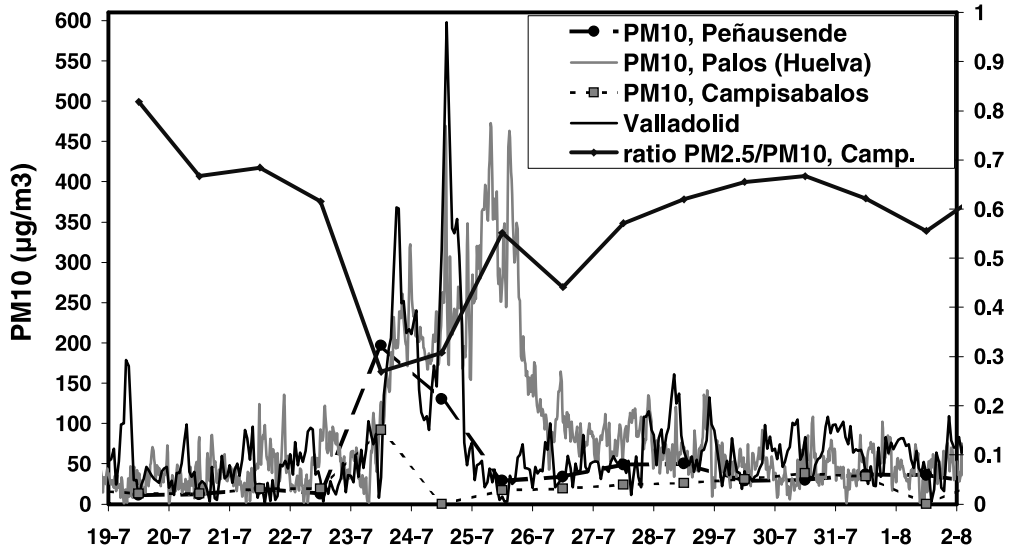

Figure 6. Time series of PM10 and the ratio PM10/PM2.5 at different stations over the IP from 19 July to 2 August 2004. (Hourly values are shown at Palos and Valladolid, and daily means are shown at Peñausende and Campisabalos, according to EMEP stations procedures.)

larger than 1 (mean value of 1.5 at this site for 4-years evaluation [*Rodrigo*, 2007]). Only after 4 August we consider the episode to be finished according to the MODIS-AOD and the Sun photometer AOD-α data.

[26] To complement the information given by the AOD-α data and quantify the impact of smoke on the AOD, we have also analyzed the predicted AOD and smoke content concentration estimated by the NAAPS Global Aerosol model (Navy Aerosol Analysis and Prediction System; available at http://www.nrlmry.navy.mil/aerosol [*Reid et al.*, 2004; *Witek et al.*, 2007]). Figure 5a, valid for 1200 UTC on each day, shows the evolution of the smoke content at ground level (μg/m^3) from 24 July to 4 August. Figure 5b displays the AOD due to smoke (in blue) and desert dust (in green). The influence of smoke over northern Spain (Palencia site) has a maximum on days 27–28 July, but extends during many days. The situation in the southwest around El Arenosillo is very similar, with the maximum on day 28 July. The NAAPS model will also be helpful in the analysis of the shape and values obtained for the volume particle size distributions (section 4.4).

4.2. Level of PM10–PM2.5 Concentration

[27] The levels of PM concentration are extraordinary and unusual, given the geographical location of the analyzed areas with respect to the source areas in Africa. We show these levels as another insight of the intensity of the event and in order to compare with AOD and column volume particle concentration. Figure 6 displays the PM10 daily values measured at Peñausende and Campisabalos, as well as the ratio PM2.5/PM10 at Campisabalos. The data show the intensity of the desert episode, with a peak on 23 July of 200 and 100 μg/m^3 respectively, and with a ratio PM2.5/PM10 about 0.3 (mean value of 0.6 during 2001–2005).

[28] Mean values at these two remote sites over the period 2001–2006 give a reference value of 13 μg/m^3 (which include the high number of desert events registered over the IP, see *Lazaridis et al.* [2006] and *Rodrigo* [2007] for details), but the background values of these sites are about 5–6 μg/m^3. Therefore during the dust event days PM10 is about 15 and 7 times this reference value respectively. The ratio PM10/PM2.5 may be used as an index for DD detection, but the data analysis in Peñausende [*Rodrigo*, 2007] shows that this ratio is a good indicator only for intense DD intrusions.

[29] Also in Figure 6 are shown the PM10 hourly values registered in two stations of ordinary high PM10 levels, Valladolid and Palos de la F. The data are very variable and the levels are spectacular, ranging from typical values (50–80 μg/m^3) to about 500 μg/m^3 at Palos and 600 μg/m^3 in Valladolid during 23–24 July. Because of the different pathway followed by the mineral dust plume to reach each station the maximum PM10 at Peñausende and Campisabalos was registered on 23 July, in Valladolid on 24 July, and in Palos de la F. on 25 July. Also note that the sampling time and the sampling technique are different which explains the different pattern or evolution for each station. After the most intense days the PM concentration does not decrease to the typical levels observed on the days before the event, but a high concentration remains until the end of the analyzed period, caused by the apportioning of smoke from the forest fires in Portugal (see the PM10 on 28 July and Figures 2 and 5).

[30] Contrasting Sun photometer columnar data and PM10 concentration helps us to evaluate the deposition time of the aerosol particles. DD intrusions arrive usually at high altitudes, about 2000–5000 m [*Molero et al.*, 2004], and are first detected by Sun photometers. The increase in the PM10 is delayed by a day or several hours, depending on the deposition process, the characteristics of the DD episode and also the sampling technique. The PM10 increased practically at the same time at Palos and Valladolid (Figure 6) although the desert plume arrived in altitude of the southern areas almost 24 h earlier.

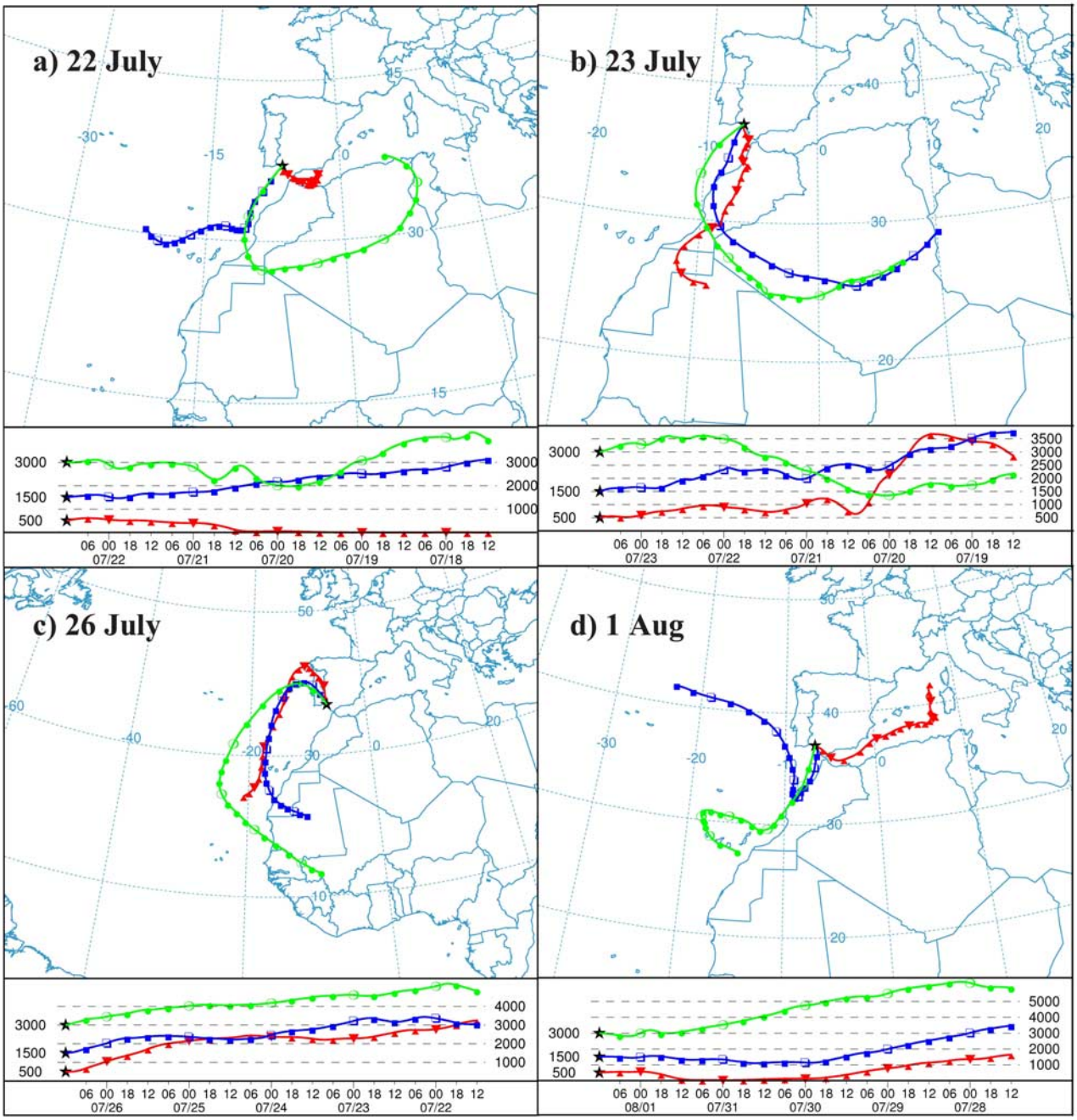

Figure 7. Back trajectories at altitudes of 500, 1500, and 3000 m over El Arenosillo station at 1200 UTC on (a) 22 July, (b) 23 July, (c) 26 July, and (d) 1 August 2004.

4.3. Meteorological Scenario: Analysis of Back Trajectories

[31] By means of the following analysis, we intend to assess the air mass origin on each day, the start and the end of the desert dust event and the type of event in terms of meteorological scenario which is responsible of the transport.

[32] As explained above from the remote sensing measurements, the dust plume arrives on 22 July in the south, at El Arenosillo (exactly on the early morning according to back trajectories), but the increase of ground particle concentration (PM10 in Palos de la F.) is detected on 23 July, 1 day later. On previous days the air mass had a clear Atlantic origin, but on 22 July (Figure 7a) the back trajectory at 3000 m at El Arenosillo arrives from North Africa, describing an anticyclone turn over the Saharan desert. However, the lower levels do not show such clear African origin yet. The next day (23 July) all the three atmospheric levels investigated (500, 1500 and 3000 m) show that the air mass origin is North Africa (Figure 7b). This situation continues, with very similar trajectories, until 25 July.

[33] Between 26 and 28 July, the air mass origin continues to be North Africa, but the back trajectories indicate a transport of the mineral dust over the Atlantic in anticyclone turn, arriving to the IP and to the measurement site El

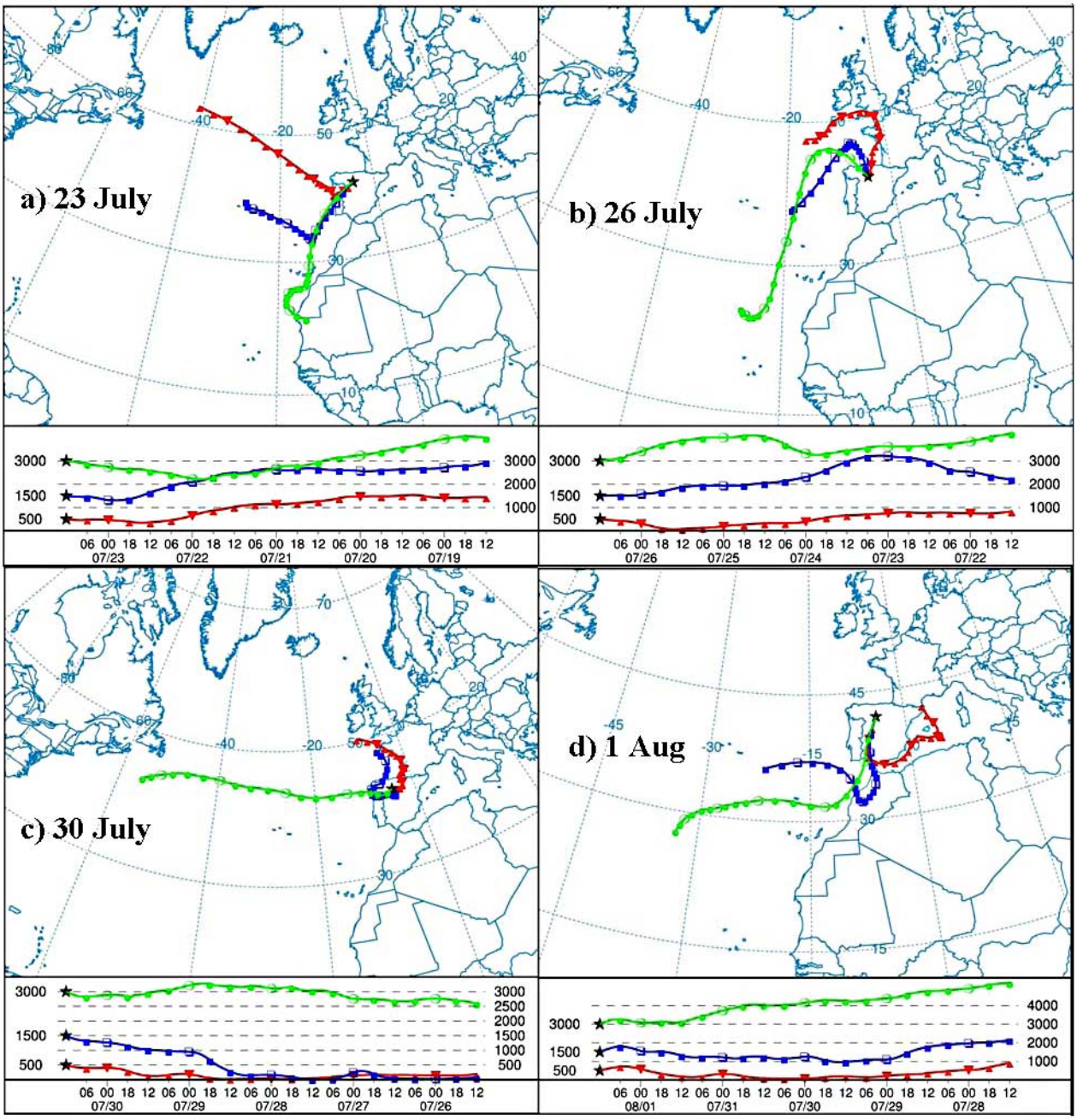

Figure 8. Same as Figure 7 for Palencia station on (a) 23 July, (b) 26 July, (c) 30 July, and (d) 1 August 2004.

Arenosillo (and also Palencia) from the northwest (Figure 7c). Because of this, the air mass travels across Portugal, where many forest fires took place, and for this reason the biomass burning aerosol is incorporated into the air mass, resulting in a very turbid atmosphere. The expected smoke concentration provided by the NAAPS model (Figure 5) is also in agreement with this, as well as the abrupt changes of the Ångström exponent (Figure 2) depending on which aerosol type predominates. The air mass on 29 and 30 July shows Atlantic or local origin, probably with smoke on 30 July (see the increase in the Ångström exponent). A new arrival of African air mass is observed after 31 July (Figure 7d), also in agreement with the AOD increase and Ångström exponent decrease at El Arenosillo (Figure 2a). On 3 August an Atlantic air mass arrived, and the typical background AOD values are obtained.

[34] About the back trajectories over the Palencia site (Figure 8), the main differences with the results in southwestern Spain are: first, the origin of the air mass is North Africa only after 23 July (1 day later than in the south). This is confirmed by the AOD observations (Figure 2b). Second, the back trajectory shows North African origin on 23–26 and 28 July, but only in the 3000 m level (Figures 8a and

8b). At low levels there is no transport of desert dust. In the period 29–31 July the trajectories show long residence time over the Iberian Peninsula (Figure 8c), therefore we find an air mass with moderate turbidity dominated by the BB aerosols (note the high Ångström exponent in Figure 2b). In this period the high atmospheric levels show Atlantic origin. The scenario changes again after 1 August, with the arrival of desert dust from North Africa (Figure 8d), as shown by an increase in the AOD and decrease in the Ångström exponent with respect to the previous days. Finally after 3 August a cleaner Atlantic advection replaces the turbid air mass.

[35] It is worth also studying the meteorological scenario which produced such a strong event. For this we will follow the analysis of meteorological scenarios described by *Escudero et al.* [2005], where 4 typical meteorological patterns for desert dust events over the Iberian Peninsula are identified. The scenario is shown in Figure 9a by means of the mean sea level pressure and geopotential height at the level of 700 hPa. It is a typical summer case, with a thermal low pressure over the Sahara due to the intense solar heating and a ridge in upper levels. Up to 10 episodes per year of this type are observed at El Arenosillo, always between May and October, with a mean duration of 4 days. The dust is present above 30% of the days between June and August [see *Toledano et al.*, 2007b, Figures 3 and 5].

[36] The strong convection produces large amounts of dust to be lifted to high altitudes, where the anticyclone turn drives them to the north. However, the high pressure in the upper levels is usually located over Tunisia or Algeria, anyway southeast of the IP, but in this episode the high pressure is clearly south of the IP, over the Sahara. From this position the dust is transported east toward the Atlantic and therefore within a plume describing an arc over the Atlantic [*Rodriguez et al.*, 2001; *Querol et al.*, 2002], see Figure 1. This kind of Atlantic arc is more typical to happen during late winter dust events. The high concentration of dust particles in summer over the Sahara traveling in a narrow plume, can be responsible for the very high AOD levels measured, especially at El Arenosillo, where the plume with AOD of 2.7 (440 nm) went over the site just in 6 h on day 22 July.

[37] The dust mobilization in the southern Saharan desert started several days before the plume was transported toward SW Europe. In Figure 9b the mean sea level pressure and 700 hPa winds on 18 July are displayed. According to this, the source region of this severe dust event was south Algeria, Niger and Mali, where the surface thermal low pressure indicates convective activity, and the strong winds in the upper levels (around 3000 m asl) indicate the transport of the dust toward the African west coast, where it is detected by the MODIS AOD already on 20 July (not shown). On 20 July a strong ridge above 750 hPa is placed over Algeria, and its opposition to the trough over the Atlantic produces strong winds in a SW–NE corridor, following the African coastline. This situation strengthens on 21 July and remains until 23 July (Figure 9a), producing the transport of the dust. The following days, the ridge in upper levels locates southwest of the IP. But again on 31 July and 1 August, when the Sun photometer data indicate the second arrival of dust, a similar scenario with ridge over Algeria and low over the Atlantic is observed.

4.4. Aerosol Particle Size Distribution and Physical Parameters

[38] Several days representative of this special DD-BB episode at El Arenosillo have been selected in order to show the main features of the Volume Size Distribution (VSD). This is illustrated in Figure 10. Because of the variability of the aerosol, it is not recommended to use daily mean values but all the available single retrievals. The particle size distributions always exhibit two modes, but the relative importance of the modes depends on the prevailing aerosol type: an accumulation or fine mode with particle radius below 0.6 μm, and a coarse mode with particle radius between 0.6 and 15 μm. Obviously we expect a predominant coarse mode during DD conditions, and more or less severe changes in this predominance depending on the influence of smoke particles, which mainly contribute to the fine mode [*Eck et al.*, 1999]. The mode radii and volume concentrations will be therefore analyzed in order to characterize the aerosol.

[39] In Figure 10a the VSD for 21 July are shown. This day is representative of relatively clean background conditions. The AOD-α values indicate a marine coastal aerosol type [*Toledano et al.*, 2007a]. The VSD on this clean day can be compared with the different VSD obtained under the influence of desert dust and smoke. Different fine and coarse mode concentrations are found in the morning and in the afternoon. During the afternoon both modes have a similar concentration, about 0.005 $\mu m^3/\mu m^2$, but in the morning the coarse mode has double concentration than the fine mode, with values about 0.02 $\mu m^3/\mu m^2$. This shows the coarse mode predominance even under relatively low AOD values. The AOD is also double in the morning than in the afternoon (see Figure 10). The fine and coarse modes are centered at 0.15 μm and 4 μm respectively.

[40] On 22–23 July the diurnal changes of the VSD are consistent with the variability already shown in the AOD-α data. Because of scattered clouds and probably to spatial inhomogeneities in the dust plume, only 3 retrievals of the VSD are available on 22 July (Figure 10b). The shape of the size distribution changes considerably with respect to the previous day, exhibiting large concentration (note the vertical scale) of the coarse mode, which is also much larger than the fine mode, in such a way that the distribution appears to be monomodal. The peak concentration reaches 1.1 $\mu m^3/\mu m^2$ (or 2.75 g/m^2, assuming particle density of 2.5 $g \cdot cm^{-3}$), the highest registered at the site, centered the coarse mode at 2.2 μm. However, the coarse mode also shows a slight prominence around 0.5–0.6 μm, indicating the existence of a secondary mode. In Figure 10b we have highlighted the fine mode in order to visualize its features and compare them with the typical conditions on 21 July. The volume concentration of the fine mode for desert aerosols is similar to the clean case and the mode radius does not vary significantly either. However, note that for two of the VSD on 22 July (those of higher concentration) the fine mode practically disappears.

[41] On 25 July (Figure 10c, and also on 24 July, not shown) the VSD exhibits well defined desert dust characteristics, with volume concentration peaks varying from 0.3 to 0.6 $\mu m^3/\mu m^2$ (or 0.75–1.5 g/m^2), and with the same shape features than the earlier days 22–23 July. During the central days of the dust episode, the AOD and VSD concentration

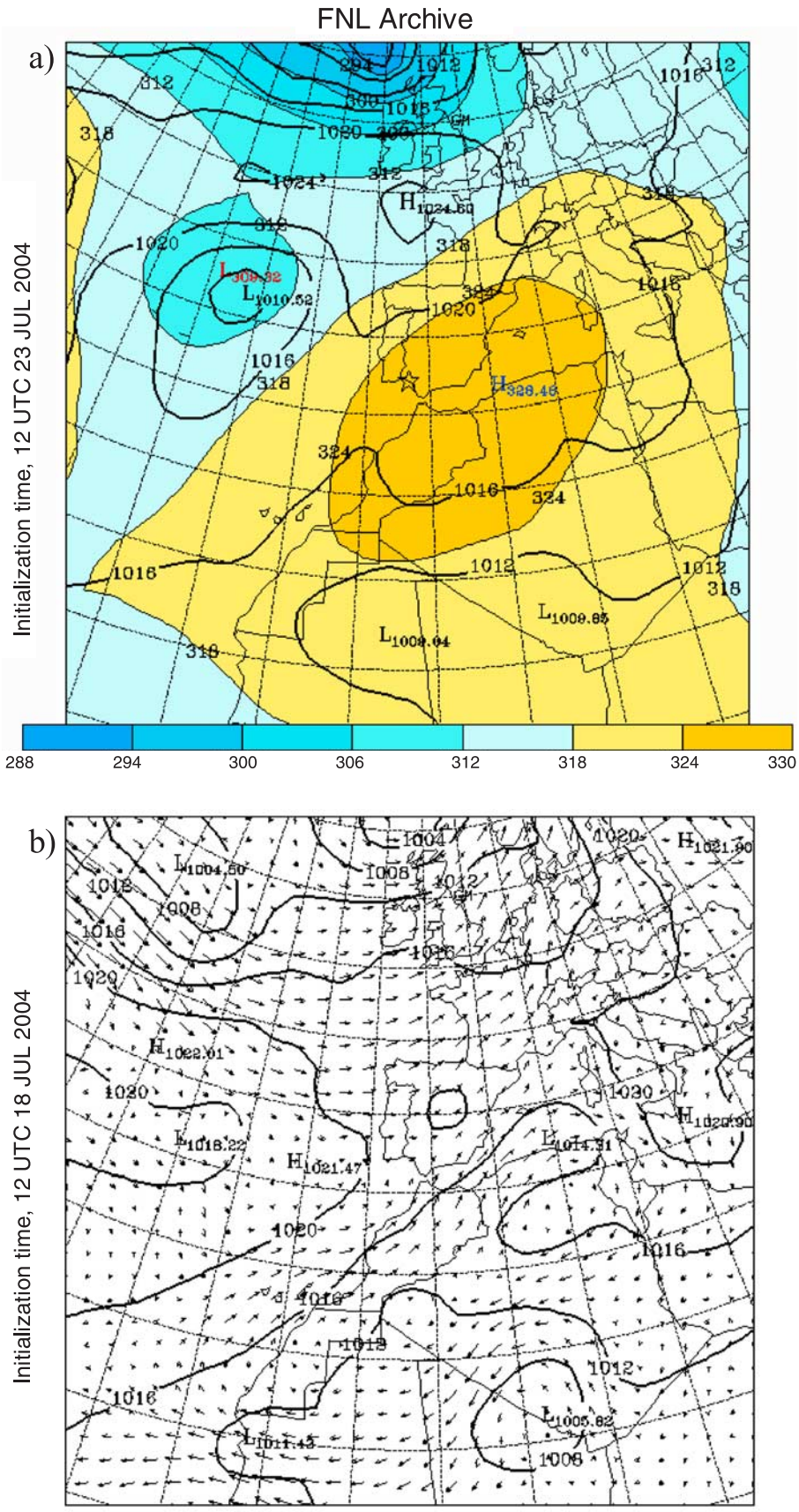

Figure 9. (a) Mean sea level pressure and geopotential height at the level of 700 hPa in southwestern Europe and North Africa on 23 July 2004. (b) FNL chart of mean sea level pressure and 700 hPa wind vectors at 1200 UTC on 18 July 2004.

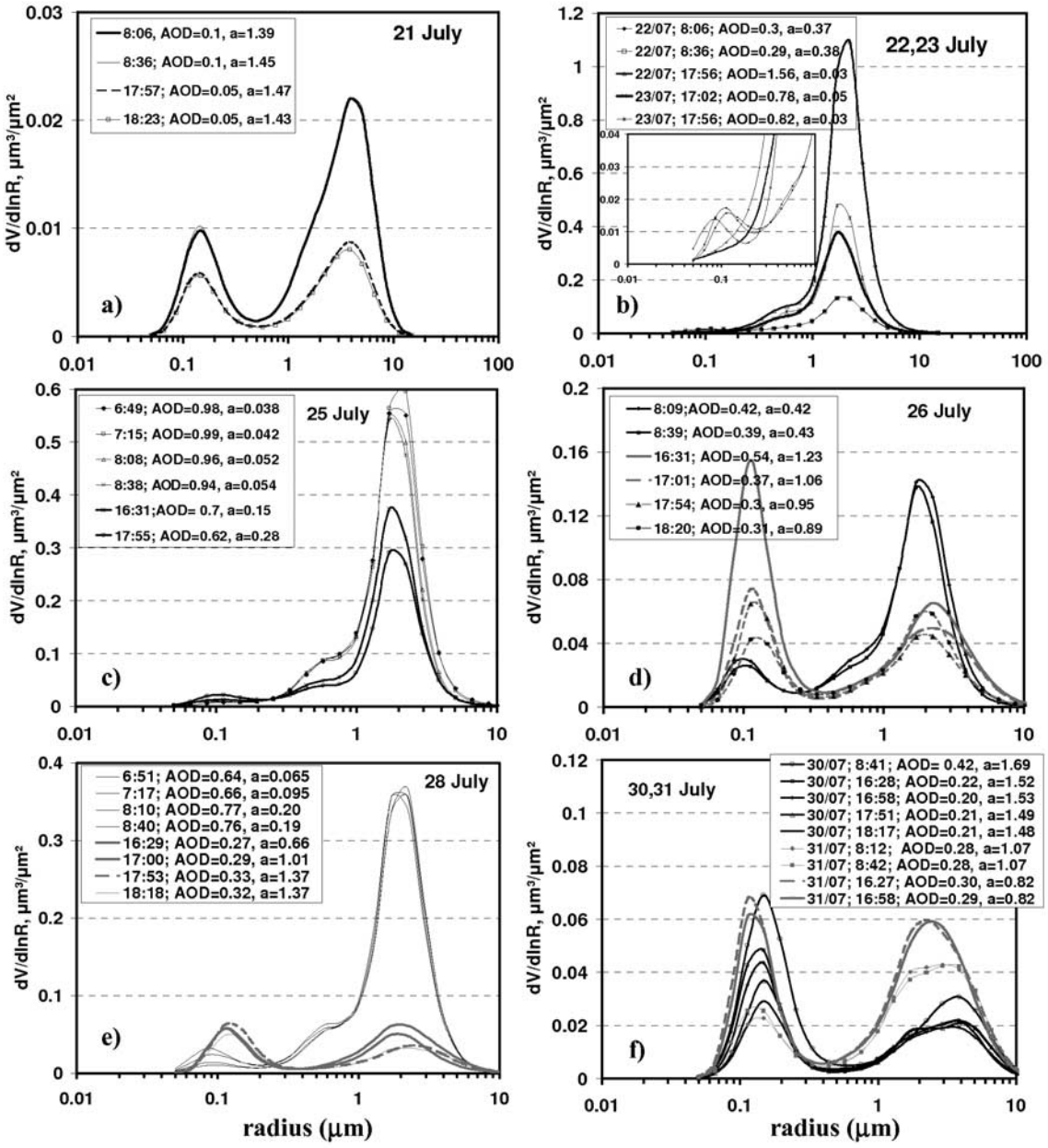

Figure 10. Volume particle size distribution given by the AERONET inversion model (version 2 and level 2.0) during the dust-smoke episode for some representative days: (a) 21 July, (b) 22 and 23 July, (c) 25 July, (d) 26 July, (e) 28 July, and (f) 30 and 31 July (measurement time and AOD-α values are reported in the panels).

values are comparable to those reported at sites with strong desert dust influence, like dust source regions [*Dubovik et al.*, 2002; *Pinker et al.*, 2001]. The morning on 26 July more typical DD aerosol conditions at El Arenosillo are observed –AOD around 0.3–0.5 and volume concentrations around 0.14 $\mu m^3/\mu m^2$ [*Cachorro et al.*, 2006; *Toledano et al.*, 2007b].

[42] During the afternoon of 26 July a different feature is observed (Figure 10d). With moderate AOD, lower than the morning values, and increase in the Ångström exponent from 0.5 to 1, the retrieved VSD are those typically obtained under smoke or industrial aerosol type [*Eck et al.*, 1999, 2005]. The first one (1631 UTC) indicates high fine mode concentration, which decreases through the afternoon. The fine-mode radius shifts slightly toward larger values respect to the DD conditions in the morning, and the same happens to the coarse mode. This is the effect of the BB plume generated in southern Portugal (Figures 4 and 5) on the aerosol size distribution.

[43] The VSD on 27–29 July (only the 28th is shown in Figure 10e) follows an equivalent behavior, with a strong desert character in the morning but with similar fine and coarse modes and lower volume concentration in the afternoon. In this latter case the fine mode radius shows a

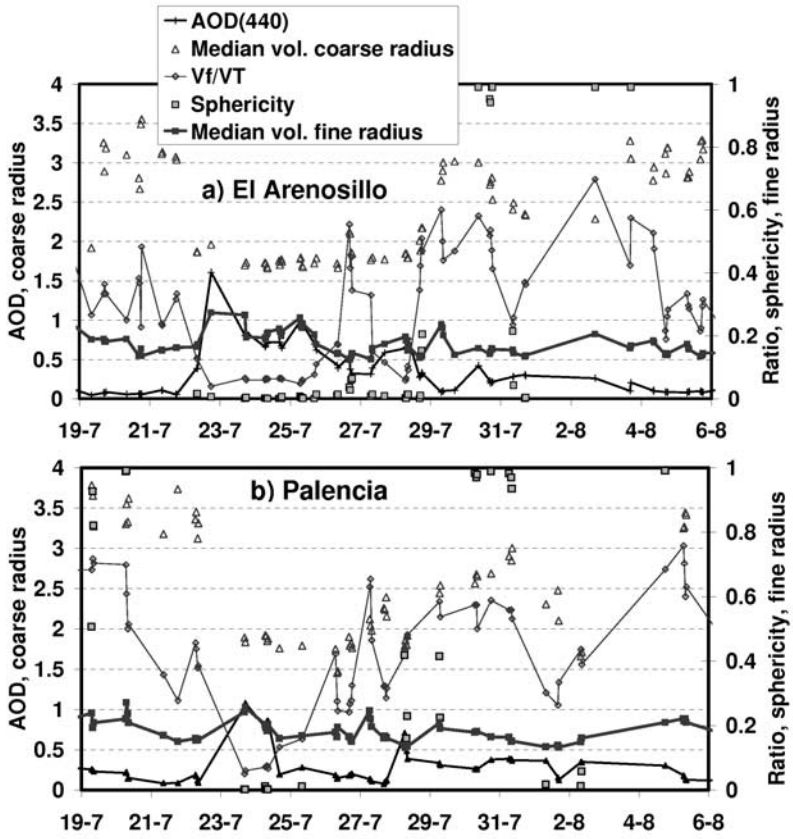

Figure 11. Time series of the AOD (440 nm), the volume median radius for fine and coarse modes, the ratio between fine mode and total volume concentration, and the sphericity parameter at (a) El Arenosillo and (b) Palencia from 19 July to 6 August 2004.

more accentuated right shift than in previous cases. This feature is especially relevant on 28 July because of the influence of the mentioned forest fire in Sierra de Aracena, in the vicinity of El Arenosillo. In the VSD obtained on 30–31 July (Figure 10f) the fine mode predominates and the desert dust seems to be absent. On 1 August a slight DD character remains, and the subsequent decrease of the AOD (3–4 August) indicates the end of this peculiar episode.

[44] The features of the VSD retrieved at the Palencia site follow a similar pattern, with clear DD character on 23–24 July and the morning on 25 July. Afterward the fine mode predominance is clearly observed, as a consequence of the mentioned forest fires in north Portugal. The data on 26 July report a mixture of DD and biomass burning aerosols, whereas on the next day (27 July) the background conditions, with typical AOD-α values at this continental site, are observed. The next days (from 27 July to 5 August) show variable conditions and great variability in the bimodal VSD but with the predominance of the fine mode (see also next Figure 11b).

[45] Figure 11 synthesizes the aerosol microphysical properties within the episode in terms of different parameters: the fine and coarse volume median radius, the ratio between the fine and total volume concentrations (V_f/V_T) and the sphericity parameter. At El Arenosillo (Figure 11a) the fine mode median radius does not change significantly (average 0.17 μm) whereas the coarse mode median radius is a good indicator of the DD arrival, falling to values around 1.8 μm. The ratio V_f/V_T also diminishes substantially to values of 0.1 during the most intense days of the DD episode. Outside these days, this ratio is very variable, although it keeps mostly below 0.5 (thus indicating coarse mode predominance) with the exception of some data corresponding to BB aerosol. For example, on 26 July the ratio increases quickly to values near 0.6, which indicates larger volume concentration of the fine or accumulation mode. The following days the ratio shows high variability

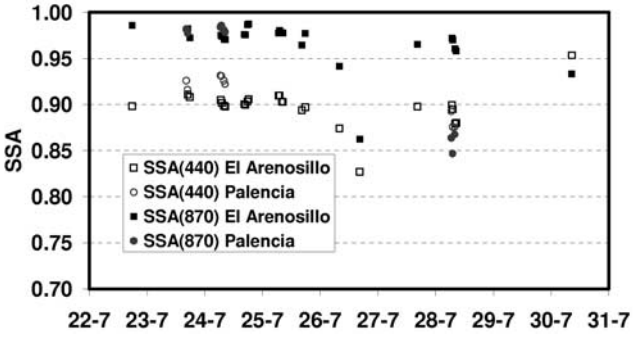

Figure 12. Time series of the SSA at 440 nm and 870 nm wavelengths at El Arenosillo and Palencia.

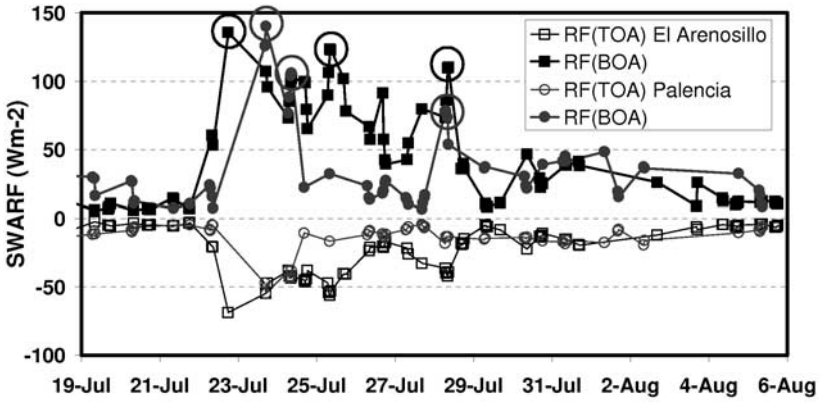

Figure 13. Time series of the instantaneous values of the shortwave aerosol direct radiative forcing (SWADRF) at the top and bottom of the atmosphere at El Arenosillo and Palencia.

(from 0.2 to 0.7), indicating the mixing and varying character of the aerosol.

[46] The sphericity parameter (given as a fraction <1) is also a useful index to characterize the aerosol type. The days before the intrusion no data are available at El Arenosillo (Figure 11a), because the measurements do not fulfill the criteria stated by AERONET for the evaluation of this parameter. On 22 July the quick arrival of the DD yields sphericity values of 0. On 26 and 28 July values near 0 are observed. The changes in the sphericity are very abrupt, and only on 28 and 31 July some intermediate values are retrieved. Out of that, either values close to 1 (in BB dominated cases) or around 0 (for the DD-predominance cases) are obtained.

[47] Figure 11b shows the equivalent parameters at the Palencia site. The main characteristic of this site is precisely the less prevalence of the coarse mode compared to El Arenosillo, both for low and moderate AOD, as shown by the values of the ratio V_f/V_T and the median volume radii. During this episode a similar behavior is observed in both sites for the days with DD character (ratio fine/total about 0.06–0.15) and those of clear BB (values about 0.6).

4.5. Single Scattering Albedo and Aerosol Direct Radiative Forcing

[48] The single scattering albedo (SSA) is a key parameter in the analysis of the aerosol radiative effects, especially in the evaluation the aerosol radiative forcing. The drawback with the SSA provided by AERONET is its high uncertainty and poor reliability. Only for AOD(440 nm) >0.4 one can rely on the accuracy on the retrieved SSA [*Dubovik et al.*, 2000]. For this reason in our areas of study, the evaluation of this parameter is only possible under high aerosol loading episodes. The SSA is illustrated in Figure 12 for 440 nm and 870 nm wavelengths, with many data at El Arenosillo site and data only on days 23–24 and 28 July at Palencia. The number of available data points is certainly limited by the (necessary) requirements of the AERONET level 2 inversion algorithm.

[49] In case of desert dust aerosol type (22–25 July) the SSA at El Arenosillo increases with wavelength, from about 0.90 at 440 nm to 0.98 at 870 nm (0.93 and 0.98 at Palencia respectively). On 26 and 28 July the SSA (440 nm) diminishes considerably to values about 0.82–0.89, indicating enhanced absorption due to the influence of smoke aerosols. However, at El Arenosillo the desert character is not lost in the whole period, since the SSA (440 nm) is smaller than SSA (870 nm), with the exception of 30 July. At Palencia on 28 July the SSA already shows inverse wavelength dependence. Despite the regional variability, the SSA for DD aerosols obtained here is within the ranges reported by other authors referring to Saharan dust [*Dubovik et al.*, 2002; *Myhre et al.*, 2003]. This is also true for the BB aerosol. For instance *Pace et al.* [2005] and *Meloni et al.* [2003] report SSA values about 0.8 for BB aerosols over some areas of Italy, because of the large and long-lasting forest fires in southern Europe during summer 2003. In the work by *Horvath et al.* [2002] an extended comparison of SSA values for many countries can be found, reporting for Europe values in the range 0.84–0.92. However, we must note the low reliability of many SSA data reported in the bibliography, especially for low AOD values and the UV spectral range. Recent publications [*Kaufman et al.*, 2001; *Haywood et al.*, 2003] emphasize the lesser absorption by desert aerosols compared with the earlier established knowledge [*World Climate Research Programme*, 1986; *D'Almeida et al.*, 1991; *Hess et al.*, 1998].

[50] The characteristics of the event are also a good opportunity to evaluate the Shortwave Aerosol Direct Radiative Forcing (SWADRF) under extreme conditions in our area. Figure 13 displays the instantaneous values of the SWADRF according to AERONET evaluation at the top of the atmosphere (TOA) and at the bottom of the atmosphere (BOA). The maxima BOA radiative forcing are 135 W/m^2 at El Arenosillo and 140 W/m^2 at Palencia, very high values compared to the typical $\approx$10 W/m^2 during nonepisodic periods. Note also the wide range of SWADRF values through the episode. Among the three highest values at the BOA (marked with a circle), the two first correspond to DD and the third corresponds to BB. The SWADRF at the TOA reaches a minimum value of -68 W/m^2 at El Arenosillo and -55 W/m^2 at Palencia during the most intense dusty conditions. Examples of representative values of the SSA (440 and 870 nm) and the radiative forcing at the TOA and BOA for dust or smoke-dominated aerosol are summarized in Table 1. Typical conditions (nonepisodic) at both sites for TOA forcing are about -4 W/m^2, but we must

Table 1. Aerosol Single Scattering Albedo and Direct Radiative Forcings (BOA and TOA) for Two Days at El Arenosillo and Palencia, Representative of Dust and Biomass Burning Aerosol[a]

Date	Type	AOD_{440}	α	SSA_{440}	SSA_{870}	RF_BOA	RF_TOA
				El Arenosillo			
23 July	dust	0.82	0.05	0.91	0.98	+107 W m^{-2}	−50 W m^{-2}
26 July	dust + smoke	0.39	1.05	0.83	0.86	+39 W m^{-2}	−21 W m^{-2}
				Palencia			
23 July	dust	1.04	0.07	0.93	0.98	+140 W m^{-2}	−55 W m^{-2}
28 July	smoke	0.53	1.35	0.88	0.86	+78 W m^{-2}	−18 W m^{-2}

[a]The AOD (440 nm) and Ångström exponent (α) are also indicated.

bear in mind the high uncertainty associated to these values because of the unreliable SSA under low AOD (the same applies to the BOA).

[51] The wide range of the SWADRF and its dependence on the AOD and the solar zenith angle (SZA) suggests calculating the radiative forcing efficiency (W m^{-2} per unit of AOD). For this purpose, a linear fit (with intercept = 0) of the SWADRF and the AOD (440 nm) is carried out (Figure 14a). The SZA varies from 53° to 75° because of the criteria used in the AERONET inversion algorithm; hence we have not considered the usual fit with AOD/cos(SZA). Figure 14a shows the data corresponding to the period 21 July to 5 August in El Arenosillo and 22 July to 5 August in Palencia. Square correlation coefficients around 0.9 or larger are obtained. The forcing efficiency at the TOA is about −55 W $m^{-2}AOD^{-1}$ at the southern site and

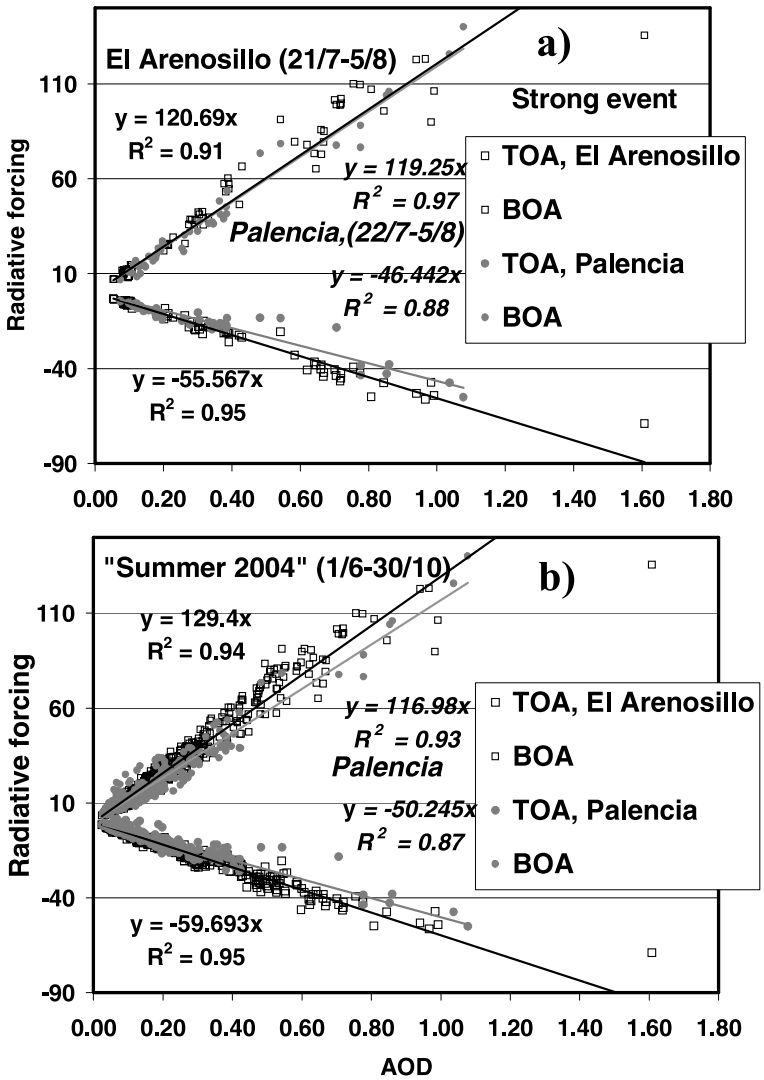

Figure 14. Linear fits of the TOA and BOA SWADRF versus the AOD(440 nm) during (a) the days of the DD-BB event at each station (El Arenosillo and Palencia) and (b) during summer 2004 (1 June to 30 October; see details in the text). Slope and square correlation coefficients for each fit are also provided. Black symbols correspond to El Arenosillo, and gray ones correspond to Palencia.

-46 W m^{-2}AOD^{-1} in the north, whereas the BOA forcing efficiency, around +120 W m^{-2}AOD^{-1}, is the same at both sites. Observe that the fit lines are far from the data points with the maximum AOD. Some low AOD data (which do not correspond to dust) are included in the fit, but no significant differences are obtained by removing these low AOD data. However, by evaluating the forcing efficiency as the mean value of all instantaneous data points (SWADRF/AOD), we obtain significant differences with the earlier result (e.g., -71 ± 14 W m^{-2}AOD^{-1} at the TOA and $+154 \pm 29$ W m^{-2}AOD^{-1} at the BOA over El Arenosillo).

[52] For further evaluation of these results, we have extended the analysis period to the entire ''summer 2004,'' which refers to a campaign lasting from 1 June to 30 October 2004. Obviously the dates do not correspond to the summer but they are representative of the summer conditions because of the high temperatures and good weather that year. This campaign was carried out at El Arenosillo for both columnar and in situ aerosol characterization [*Prats et al.*, 2008]. The summer 2004 registered very frequent and intense DD intrusions [*Toledano et al.*, 2007b]. The AOD-radiative forcing fits for this period are illustrated in Figure 14b for El Arenosillo and Palencia, although the inventory of DD events is different for each site. The results are close to those reported for other DD episodes of comparable AOD [*Haywood et al.*, 2003; *Myhre et al.*, 2003; *Liu et al.*, 2003; *Li et al.*, 2004]. The aerosol radiative forcing evaluated over other sites in the IP is not directly comparable with this case study because of the different aerosol conditions, spectral range or methodology used [e.g., *Horvath et al.*, 2002; *Diaz et al.*, 2007]. However, these values show that DD outbreaks and BB episodes have an important impact over our study area and must be accounted for in the evaluation of local-regional climatic scenarios. Furthermore, an inventory of BB over the IP and its radiative impact appears to be a necessary work to be accomplished because of the high occurrence of large forest fires in the last years.

5. Conclusions

[53] We have carried out a detailed analysis of columnar aerosol properties over two AERONET sites in Spain, representative of two climatic areas, during a special episode which affected the entire Iberian Peninsula. During the analyzed period the strongest desert dust intrusion reported up-to-date over the IP took place, and at the same time the atmosphere was influenced by biomass burning aerosol from forest fires, very frequent in summer in this region. The AERONET sites provide a set of aerosol parameters which allow a complete characterization of the aerosols, including the evaluation of the direct radiative forcing. Very important in this case study is to report the range of values of different aerosol parameters: spectral AOD, Ångström exponent, volume fine and coarse concentration and mode radius. Together with these parameters, the SSA appears as a challenging parameter because of the high uncertainty associated with its determination and its critical importance for an accurate aerosol radiative forcing evaluation. The aerosol scenario (aerosol types, microphysical and optical properties) represented by this extreme episode of DD-BB constitutes a relevant reference to be accounted for in the estimation of the aerosol forcing impact in areas like southern Europe, which appear as more sensitive to climate change.

[54] **Acknowledgments.** Financial support for this work was given by CICYT and the Government of Castilla y León region. The Cimel photometers whose data are used in this publication belong to the AERONET-PHOTONS network and the Spanish federated RIMA network; we thank all the people involved in these programs. The authors also thank Garcia Perez from the Environmental Office of the AQN of Valladolid, A. González Ortiz of the Environmental Office of Spain MMA for the EMEP stations data, and J. A. Adame of INTA for providing PM data of Andalusia regional network. The authors gratefully acknowledge the NOAA Air Resources Laboratory (ARL) for the provision of the HYSPLIT transport and dispersion model and READY website used in this publication. Thanks are also due to the NRL for the provision of the NAAPS model, to the SeaWIFS and MODIS teams of NASA, and to LATUV for the satellite data used in this publication.

References

Avila, A. (1999), Las lluvias de barro y el transporte y deposición de material sahariano sobre el nordeste de la península ibérica, *Orsis*, *14*, 105–127.

Avila, A., I. Queralt-Mitjans, and M. Alarcón (1997), Mineralogical composition of African dust delivered by red rains over northeastern Spain, *J. Geophys. Res.*, *102*(D18), 21,977–21,996, doi:10.1029/97JD00485.

Cachorro, V. E., A. M. de Frutos, and J. L. Casanova (1987), Determination of Ångström turbidity parameters, *Appl. Opt.*, *26*, 3069–3076.

Cachorro, V. E., R. Vergaz, A. M. De Frutos, J. M. Vilaplana, D. Henriques, N. Laulainen, and C. Toledano (2006), Study of desert dust events over the southwestern Iberian Peninsula in year 2000: Two case studies, *Ann. Geophys.*, *24*, 1–18.

Chiapello, I., C. Moulin, and J. M. Prospero (2005), Understanding the long-term variability of African dust transport across the Atlantic as recorded in both Barbados surface concentrations and large-scale Total Ozone Mapping Spectrometer (TOMS) optical thickness, *J. Geophys. Res.*, *110*, D18S10, doi:10.1029/2004JD005132.

D'Almeida, G. A., P. Koepke, and E. P. Shettle (1991), *Atmospheric Aerosol: Global Climatology and Radiative Characteristics*, A. Deepak, Hampton, Va.

Diaz, A. M., et al. (2007), Aerosol radiative forcing efficiency in the UV region over southeastern Mediterranean: VELETA2002 campaign, *J. Geophys. Res.*, *112*, D06213, doi:10.1029/2006JD007348.

Draxler, R., and G. Rolph (2003), HYSPLIT (Hybrid Single-Particle Lagrangian Integrated Trajectory) model, Air Resour. Lab., NOAA, Silver Spring, Md. (Available at http://www.arl.noaa.gov/ready/hysplit4.html)

Dubovik, O., and M. King (2000), A flexible inversion algorithm for retrieval of aerosol optical properties from Sun and sky radiance measurements, *J. Geophys. Res.*, *105*(D16), 20,673–20,696, doi:10.1029/2000JD900282.

Dubovik, O., A. Smirnov, B. N. Holben, M. D. King, Y. J. Kaufman, T. F. Eck, and I. Slutsker (2000), Accuracy assessments of aerosol optical properties retrieved from AERONET Sun and sky-radiance measurements, *J. Geophys. Res.*, *105*, 9791–9806, doi:10.1029/2000JD900040.

Dubovik, O., B. N. Holben, T. F. Eck, A. Smirnov, Y. J. Kaufman, M. D. King, D. Tanre, and I. Slutsker (2002), Variability of absorption and optical properties of key aerosol types observed in worldwide locations, *J. Atmos. Sci.*, *59*, 590–608, doi:10.1175/1520-0469(2002)059<0590:VOAAOP>2.0.CO;2.

Dubovik, O., et al. (2006), Application of spheroid models to account for aerosol particle nonsphericity in remote sensing of desert dust, *J. Geophys. Res.*, *111*, D11208, doi:10.1029/2005JD006619.

Eck, T. F., B. N. Holben, J. S. Reid, O. Dubovik, A. Smirnov, N. T. O'Neill, I. Slutsker, and S. Kinne (1999), The wavelength dependence of the optical depth of biomass burning, urban and desert dust aerosols, *J. Geophys. Res.*, *104*, 31,333–31,350.

Eck, T. F., et al. (2005), Columnar aerosol optical properties at AERONET sites in central eastern Asia and aerosol transport to the tropical mid-Pacific, *J. Geophys. Res.*, *110*, D06202, doi:10.1029/2004JD005274.

Escudero, M., S. Castillo, X. Querol, A. Avila, M. Alarcón, M. M. Viana, A. Alastuey, E. Cuevas, and S. Rodríguez (2005), Wet and dry African dust episodes over eastern Spain, *J. Geophys. Res.*, *110*, D18S08, doi:10.1029/2004JD004731.

Escudero, M., A. Stein, R. R. Draxler, X. Querol, A. Alastuey, S. Castillo, and A. Avila (2006), Determination of the contribution of northern Africa dust source areas to PM10 concentrations over the central Iberian Peninsula using the Hybrid Single-Particle Lagrangian Integrated Trajectory

model (HYSPLIT) model, *J. Geophys. Res.*, *111*, D06210, doi:10.1029/2005JD006395.

Garcia-Herrera, R., J. Diaz, R. M. Trigo, and E. Hernández (2005), Extreme summer temperatures in Iberia: Health impacts and associated synoptic conditions, *Ann. Geophys.*, *23*, 239–251, sref:1432-0576/ag/2005-23-239.

Ginoux, P., J. M. Prospero, O. Torres, and M. Chin (2004), Long-term simulation of global dust distribution with the GOCART model: Correlation with North Atlantic Oscillation, *Environ. Model. Softw.*, *19*(2), 113–128, doi:10.1016/S1364-8152(03)00114-2.

González, Y., J. De la Rosa, A. M. Sánchez de la Campa, A. Alastuey, X. Querol, J. P. Bolivar, V. Cachorro, and M. Sorribas (2007), Levels of chemical composition of PM10 and PM2.5 in "El Arenosillo" rural monitoring station (SW Spain), paper presented at European Aerosol Conference, Eur. Aerosol Assem., Salzburg, Austria.

Goudie, A., and N. Middleton (2001), Saharan dust storms: Nature and consequences, *Earth Sci. Rev.*, *56*, 179–204, doi:10.1016/S0012-8252(01)00067-8.

Haywood, J., P. Francis, S. Osborne, M. Glew, N. Loeb, E. Highwood, D. Tanré, G. Myhre, P. Formenti, and E. Hirst (2003), Radiative properties and direct radiative effect of Saharan dust measured by the C-130 aircraft during SHADE: 1. Solar spectrum, *J. Geophys. Res.*, *108*(D18), 8577, doi:10.1029/2002JD002687.

Hess, M., P. Koepke, and I. Schult (1998), Optical properties of aerosols and clouds: The software package OPAC, *Bull. Am. Meteorol. Soc.*, *79*(5), 831–844, doi:10.1175/1520-0477(1998)079<0831:OPOAAC>2.0.CO;2.

Holben, B. N., et al. (1998), AERONET—A federated instrument network and data archive for aerosol characterization, *Remote Sens. Environ.*, *66*(1), 1–16, doi:10.1016/S0034-4257(98)00031-5.

Holben, B. N., et al. (2001), An emerging ground-based aerosol climatology: Aerosol optical depth from AERONET, *J. Geophys. Res.*, *106*, 12,067–12,097, doi:10.1029/2001JD900014.

Horvath, H., L. Alados-Arboledas, F. J. Olmo, O. Jovanovie, M. Gang, W. Kaller, C. Sánchez, H. Sauerzopf, and S. Seidl (2002), Optical characteristics of the aerosol in Spain and Austria and its effect on radiative forcing, *J. Geophys. Res.*, *107*(D19), 4386, doi:10.1029/2001JD001472.

Kaufman, Y. J., D. Tanré, O. Dubovik, L. A. Karnieri, and L. A. Remer (2001), Absorption of sunlight by dust as inferred by satellite and ground-based remote sensing, *Geophys. Res. Lett.*, *28*, 1479–1482, doi:10.1029/2000GL012647.

Kaufman, Y. J., I. Koren, L. A. Remer, D. Tanré, P. Ginoux, and S. Fan (2005), Dust transport and deposition observed from the Terra-Moderate Resolution Imaging Spectrometer (MODIS) spacecraft over the Atlantic Ocean, *J. Geophys. Res.*, *110*, D10S12, doi:10.1029/2003JD004436.

Lazaridis, M., I. Kopanakis, V. Cachorro, K. Espen, and W. Aas (2006), Measurements of particulate matter (PM10, PM2.5 and PM1) in 2004, in *Measurements of Particulate Matter: Status Report 2006*, *EMEP/CCC-Rep. 3/2006*, pp. 11–40, Norw. Inst. for Air Res., Kjeller, Norway.

Li, F., A. M. Vogelmann, and V. Ramanathan (2004), Saharan Dust aerosol radiative forcing measured from space, *J. Clim.*, *17*, 2558–2571, doi:10.1175/1520-0442(2004)017<2558:SDARFM>2.0.CO;2.

Liu, X., J. Wuag, and S. A. Christopher (2003), Shortwave direct radiative forcing of Saharan dust aerosols over the Atlantic ocean, *Int. J. Remote Sens.*, *24*, 1–15, doi:10.1080/143116031000114824.

Lyamani, H., F. J. Olmo, A. Alcantara, and L. Alados-Arboledas (2006), Atmospheric aerosols during the 2003 heat wave in southeastern Spain II: Microphysical columnar properties and radiative impact, *Atmos. Environ.*, *40*, 6465–6476, doi:10.1016/j.atmosenv.2006.04.047.

Meloni, D., A. di Sarra, J. de Luisi, T. Di Iorio, G. Fiocco, W. Junkerman, and G. Pace (2003), Tropospheric aerosols in the Mediterranean: 2. Radiative effects through model simulation and measurements, *J. Geophys. Res.*, *108*(D10), 4317, doi:10.1029/2002JD002807.

Millán, M. M., R. Salvador, and E. Mantilla (1997), Photo-oxidant dynamic in the Mediterranean Basin in summer: Results from European research projects, *J. Geophys. Res.*, *102*, 8811–8823, doi:10.1029/96JD03610.

Molero, F., et al. (2004), Characterization of a Saharan dust event during Veleta-2002 (Spain) campaign, in *Proceedings of the 22nd International Laser Radar Conference (ILRC 2004)*, edited by G. Papalardo and A. Amodeo, *Eur. Space Agency Spec. Publ.*, *ESA SP-561*, 531–534.

Mona, L., A. Amodeo, M. Pandolfi, and G. Pappalardo (2006), Saharan dust intrusions in the Mediterranean area: Three years of Raman lidar measurements, *J. Geophys. Res.*, *111*, D16203, doi:10.1029/2005JD006569.

Myhre, G., A. Grini, J. M. Haywood, F. Stordal, B. Chatenet, D. Tanré, J. K. Sundet, and I. S. A. Isaksen (2003), Modeling the radiative impact of mineral dust during the Saharan Dust Experiment (SHADE) campaign, *J. Geophys. Res.*, *108*(D18), 8579, doi:10.1029/2002JD002566.

Pace, G., D. Meloni, and A. di Sarra (2005), Forest fire aerosols over the Mediterranean basin during summer 2003, *J. Geophys. Res.*, *110*, D21202, doi:10.1029/2005JD005986.

Pace, G., A. di Sarra, D. Meloni, S. Piacentino, and P. Chamard (2006), Optical properties of aerosols over the central Mediterranean. 1. Influence of transport and identification of different aerosol types, *Atmos. Chem. Phys.*, *6*, 697–713.

Perez, C., S. Nickovic, J. M. Baldasano, M. Sicard, F. Rocadenbosch, and V. E. Cachorro (2006), A long Saharan dust event over the western Mediterranean: Lidar, Sun photometer observations, and regional dust modeling, *J. Geophys. Res.*, *111*, D15214, doi:10.1029/2005JD006579.

Pinker, R., G. Pandithurai, B. Holben, O. Dubovik, and T. Aro (2001), A dust outbreak in sub-Sahel West Africa, *J. Geophys. Res.*, *106*, 22,923–22,930, doi:10.1029/2001JD900118.

Prats, N., V. E. Cachorro, M. Sorribas, S. Mogo, A. Berjón, C. Toledano, A. M. de Frutos, J. de la Rosa, N. Laulainen, and B. A. de la Morena (2008), Characterization of the aerosol columnar microphysical and radiative properties during "El Arenosillo 2004 summer campaign," *Atmos. Environ.t*, *42*, 2643–2653.

Prospero, J. M., P. Ginoux, O. Torres, S. E. Nicholson, and T. E. Gill (2002), Environmental characterization of global sources of atmospheric soil dust identified with the NIMBUS 7 Total Ozone Mapping Spectrometer (TOMS) absorbing aerosol product, *Rev. Geophys.*, *40*(1), 1002, doi:10.1029/2000RG000095.

Querol, X., S. Rodríguez, E. Cuevas, M. M. Viana, and A. Alastuey (2002), Intrusiones de masas de aire africano sobre la Península Ibérica y Canarias: Mecanismos de transporte y variación estacional, paper presented at 3ª Asamblea Hispano Portuguesa de Geodesia y Geofísica, Com. Esp. de Geod. y Geofis., Valencia, Spain.

Querol, X., et al. (2004), Levels of particulate matter in rural, urban and industrial sites in Spain, *Sci. Total Environ.*, *334–335*, 359–376.

Querol, X., J. de la Rosa, and A. Sánchez de la Campa (2008), Spatial and temporal variations in airborne particulate matter (PM10 and PM2.5) across Spain 1999–2005, *Atmos. Environ.*, *42*(17), 3964–3979.

Reid, J. S., E. M. Prins, D. L. Westphal, C. C. Schmidt, K. A. Richardson, S. A. Christopher, T. F. Eck, E. A. Reid, C. A. Curtis, and J. P. Hoffman (2004), Real-time monitoring of South American smoke particle emissions and transport using a coupled remote sensing/box-model approach, *Geophys. Res. Lett.*, *31*, L06107, doi:10.1029/2003GL018845.

Rodrigo, R. (2007), Detección, caracterización y evaluación de aerosoles en la Comunidad de Castilla y León, predoctoral work (DEA), Univ. de Valladolid, Valladolid, Spain.

Rodriguez, S., X. Querol, A. Alastuey, G. Kallos, and O. Kakaliagou (2001), Saharan dust contributions to PM10 and TSP levels in southern and eastern Spain, *Atmos. Environ.*, *35*, 2433–2447, doi:10.1016/S1352-2310(00)00496-9.

Rodriguez, S., X. Querol, A. Alastuey, and E. Mantilla (2002), Origin of high summer PM10 and TSP concentrations at rural sites in eastern Spain, *Atmos. Environ.*, *36*, 3101–3112, doi:10.1016/S1352-2310(02)00256-X.

Rolph, G. D. (2003), Real-time Environmental Applications and Display System (READY), Air Resour. Lab., NOAA, Silver Spring, Md. (Available at http://www.arl.noaa.gov/ready/hysplit4.html)

Sokolik, I. N., D. M. Winker, G. Bergametti, D. A. Gillette, G. Carmichael, Y. J. Kaufman, L. Gomes, L. Schuetz, and J. E. Penner (2001), Introduction to special section: Outstanding problems in quantifying the radiative impacts of mineral dust, *J. Geophys. Res.*, *106*, 18,015–18,027.

Sorribas, M., V. E. Cachorro, S. Mogo, A. M. de Frutos y, and B. A. de la Morena (2006), General Characterization of the Monitoring Station of the "in situ" Atmospheric Aerosols Properties at El Arenosillo, paper presented at 5ª Asamblea Hispano-Portuguesa de Geodesia y Geofísica, Com. Esp. de Geod. y Geofis., Sevilla, Spain.

Stunder, B. (1997), NCEP model output—FNL archive data, Air Resour. Lab., NOAA, Silver Spring, Md. (Available at http://www.arl.noaa.gov/ss/transport/archives.html)

Tanré, D., J. Haywood, J. Pelon, J. Leon, B. Chatenet, P. Formenti, P. Francis, P. Goloub, E. Highwood, and G. Myhre (2003), Measurement and modeling of the Saharan dust radiative impact: Overview of the Saharan Dust Experiment (SHADE), *J. Geophys. Res.*, *108*(D18), 8574, doi:10.1029/2002JD003273.

Toledano, C., V. E. Cachorro, M. Sorribas, A. Berjón, B. A. de la Morena, A. M. de Frutos, and P. Gouloub (2007a), Aerosol optical depth and Ångström exponent climatology at El Arenosillo AERONET site (Huelva, Spain), *Q. J. R. Meteorol. Soc.*, *133*, 795–807, doi:10.1002/qj.54.

Toledano, C., V. E. Cachorro, A. M. de Frutos, M. Sorribas, N. Prats, and B. A. de la Morena (2007b), Inventory of African desert dust events over the southwestern Iberian Peninsula in 2000–2005 with an AERONET Cimel Sun photometer, *J. Geophys. Res.*, *112*, D21201, doi:10.1029/2006JD008307.

Witek, M. L., P. J. Flatau, P. K. Quinn, and D. L. Westphal (2007), Global sea-salt modeling: Results and validation against multicampaign shipboard measurements, *J. Geophys. Res.*, *112*, D08215, doi:10.1029/2006JD007779.

World Climate Research Programme (1986), A preliminary cloudless standard atmosphere for radiation computation, *Rep. 112*, Geneva, Switzerland.

A. Berjón, V. E. Cachorro, A. M. De Frutos, N. Prats, R. Rodrigo, and B. Torres, Group of Atmospheric Optics, University of Valladolid, E-47071 Valladolid, Spain.

J. de la Rosa, Department of Geology, University of Huelva, E-21071 Huelva, Spain.

S. Mogo, Departamento de Fisica, Universidad da Beira Interior, P-6201-001 Covilhã, Portugal.

M. Sorribas, Estación de Sondeos Atmosféricos El Arenosillo, Ctra. San Juan del Puerto-Matalascañas, Km. 33, E-21130 Mazagón, Spain.

C. Toledano, Meteorological Institute, University of Munich, D-80333 Munich, Germany. (toledano@baraja.opt.cie.uva.es)